Redox Biology 49 (2022) 102207

Contents lists available at ScienceDirect

Redox Biology

journal homepage: www.elsevier.com/locate/redox

Porcine reproductive and respiratory syndrome virus nsp4 positively regulates cellular cholesterol to inhibit type I interferon production

Wenting Ke [a,b,1], Yanrong Zhou [a,b,1], Yinan Lai [a,b], Siwen Long [a,b], Liurong Fang [a,b,**], Shaobo Xiao [a,b,*]

[a] State Key Laboratory of Agricultural Microbiology, College of Veterinary Medicine, Huazhong Agricultural University, Wuhan, 430070, China
[b] The Key Laboratory of Preventive Veterinary Medicine in Hubei Province, Cooperative Innovation Center for Sustainable Pig Production, Wuhan, 430070, China

ARTICLE INFO

Keywords:
PRRSV
Cholesterol
PP2A
AMPK
HMGCR
Interferon

ABSTRACT

Cellular cholesterol plays an important role in the life cycles of enveloped viruses. Previous studies by our group and other groups have demonstrated that the depletion of cellular cholesterol by methyl-β-cyclodextrin (MβCD) reduces the proliferation of porcine reproductive and respiratory syndrome virus (PRRSV), a porcine *Arterivirus* that has been devastating the swine industry worldwide for over two decades. However, how PRRSV infection regulates cholesterol synthesis is not fully understood. In this study, we showed that PRRSV infection upregulated the activity of protein phosphatase 2 (PP2A), which subsequently activated 3-hydroxy-3-methylglutaryl coenzyme A reductase (HMGCR), the rate-limiting enzyme in the cholesterol synthesis pathway, to increase the levels of cellular cholesterol. By screening the PRRSV-encoded proteins, we showed that nsp4 dominated the upregulation of cellular cholesterol, independently of the 3C-like protease activity of nsp4. A mutation analysis showed that domain I (amino acids 1–80) of PRRSV nsp4 interacted with PR65 alpha (PR65α), the structural subunit, and PP2Ac, the catalytic subunit, of PP2A. Importantly, domain I of nsp4 inhibited Sendai virus-induced interferon β production, and this inhibitory effect was eliminated by Lovastatin, an HMGCR inhibitor, indicating that the upregulation of cellular cholesterol by nsp4 is a strategy used by PRRSV to suppress the antiviral innate immunity of its host. Collectively, we here demonstrated the mechanism by which PRRSV regulates cellular cholesterol synthesis and reported a novel strategy by which PRRSV evades its host's antiviral innate immune response.

1. Introduction

Since it was first reported in the 1980s, porcine reproductive and respiratory syndrome (PRRS) has been one of the most economically significant swine diseases worldwide [1,2]. The causative agent, porcine reproductive and respiratory syndrome virus (PRRSV), is an enveloped virus with a single-stranded, positive-sense RNA genome of nearly 15 kb, belonging to the order *Nidovirales* in the family *Arteriviridae* [3–6]. During PRRSV infection, two viral replicase polyproteins, pp1a and pplab, encoded by open reading frame 1a (ORF1a) and ORF1b, respectively, are cleaved into 14 mature nonstructural proteins (nsps) by viral proteases (nsp1α, nsp1β, nsp2, and nsp4) [7–9]. The other ORFs encode eight structural proteins, including glycoprotein (GP) 2, envelope (E) protein, GP3, GP4, GP5, ORF5a protein, membrane (M) protein, and nucleocapsid (N) protein [10–12], and two nsps, including nsp2TF and nsp2N [13,14]. PRRSV is an evolutionarily successful virus that uses elaborate strategies to evade the antiviral immune responses of its host. One is the inhibition of interferon (IFN) response, which is mediated by multiple viral proteins, particularly nsp4. Nsp4 is the viral main protease, and uses a 3C-like protease (3CLP) activity to cleave the viral polyproteins and host factors involved in the innate immune responses [15–19]. PRRSV also regulates the host's metabolism, for example, disturbing the biosynthesis of lipids [20,21] and polyamine [22], to establish a chronic persistent infection.

* Corresponding author. State Key Laboratory of Agricultural Microbiology, College of Veterinary Medicine, Huazhong Agricultural University, Wuhan, 430070, China.
** Corresponding author. State Key Laboratory of Agricultural Microbiology, College of Veterinary Medicine, Huazhong Agricultural University, Wuhan, 430070, China.
E-mail addresses: fanglr@mail.hzau.edu.cn (L. Fang), vet@mail.hzau.edu.cn (S. Xiao).
[1] These authors contributed equally.

https://doi.org/10.1016/j.redox.2021.102207
Received 3 November 2021; Received in revised form 26 November 2021; Accepted 7 December 2021
Available online 8 December 2021

Cholesterol is an important component of cellular membrane and plays an important role in the proliferation of viruses that require biological membranes to establish their infection. Replication complexes (RCs), which act as platforms for viral replication and the production of progeny virions, are partially isolated compartments that form from the endoplasmic reticulum membrane during the infection processes of many viruses [23,24]. Cholesterol helps to maintain the stability and fluidity of biological membranes, so it is required for the formation of RCs, explaining the involvement of cholesterol in the infection processes of these viruses. Moreover, the receptors that mediate the absorption and invasion processes of many viruses occur in lipid rafts, the cholesterol-rich microdomains in the plasma membrane [25,26], supporting the association between viral infection and cholesterol homeostasis. Therefore, it is not surprising that viruses have developed different strategies to regulate cholesterol metabolism. Because the enzyme 3-hydroxy-3-methylglutaryl coenzyme A reductase (HMGCR) is the rate-limiting enzyme in the synthesis of cholesterol [27], a number of viruses modulate cholesterol synthesis by targeting HMGCR through various mechanisms, such as Kaposi's sarcoma-associated herpesvirus [28], Hepatitis B virus (HBV) [29], Flaviviruses [30], and Human cytomegalovirus [31]. The activity of HMGCR is mainly regulated through its phosphorylation, predominantly by two upstream molecules, adenosine 5′-monophosphate-activated protein kinase (AMPK) and protein phosphatase 2A (PP2A). AMPK phosphorylates HMGCR (inactive form) and PP2A dephosphorylates it (active form) [32,33]. Thus, the activity of AMPK is also altered by some viruses to provide a favorable lipid environment for their proliferation, such as Porcine circovirus type 2 (PCV2) [34,35], and Dengue virus (DENV) [36,37]. However, there have been few studies regarding the role of PP2A in virus-regulated cholesterol metabolism.

Emerging evidences support a close relationship between the innate immune system and cholesterol metabolism [38,39]. The reduction of cholesterol synthesis in macrophages is accompanied by the activation of the STING–TBK1–IRF3 pathway, which induces the production of type I IFN (IFN-I) [40], suggesting that the inhibition of cholesterol synthesis activates the IFN-I response. Cholesterol-25-hydroxylase (CH25H), the expression of which is induced by IFN treatment, converts cholesterol to 25-hydroxycholesterol (25HC), causing a reduction in intracellular cholesterol. Notably, 25HC is a recently identified naturally occurring oxysterol, which exerts antiviral activity against a broad range of viruses. These findings indicate that IFN inhibits viral infection by reducing cholesterol levels. IFN-induced transmembrane proteins 3 has been shown to antagonize PRRSV membrane fusion by disturbing intracellular cholesterol homeostasis [41]. However, the regulatory mechanisms and possible relationship between cellular cholesterol and the innate immune response during PRRSV infection remain unclear.

In this study, we demonstrated that PRRSV infection upregulated the activity of HMGCR by targeting PP2A, thus inducing the synthesis of cholesterol. Mechanistically, PRRSV nsp4 interacted with PP2A, resulting in the reduction of PP2A phosphorylation (inactive form), which up-regulated cholesterol levels through decreasing HMGCR phosphorylation. Significantly, nsp4-induced cholesterol biosynthesis upregulation partly accounted for nsp4-mediated IFN-β inhibition.

2. Materials and methods

2.1. Materials

Primary porcine alveolar macrophages (PAMs), the main target cells of PRRSV *in vivo*, were isolated from the lungs of 30-day-old healthy piglets and cultured in RPMI-1640 (Sigma-Aldrich, USA). PK-15^{CD163} cells, a pig kidney cell line stably expressing the PRRSV receptor CD163, and HEK-293T cells were cultured in Dulbecco's modified Eagle's medium (DMEM; Invitrogen, USA). All cells were cultured in medium supplemented with 10% fetal bovine serum (FBS; Gibco, USA) at 37 °C under a humidified atmosphere containing 5% CO_2. PRRSV strain WUH3 is a highly pathogenic type 2 (North American) virus isolated in 2006 from the brains of pigs suffering from "high-fever syndrome" in China [42]. PRRSV was amplified and titered in PK-15^{CD163} cells and PAMs.

Mouse or rabbit monoclonal antibodies (mAbs) directed against Flag, HA, GFP, and β-actin were purchased from Medical and Biological Laboratories (MBL, Japan). Rabbit polyclonal antibodies (pAbs) directed against p-AMPK and AMPK were purchased from Cell Signaling Technology (CST, USA). Rabbit pAbs directed against p-HMGCR and HMGCR were purchased from Abcam (UK) and Abmart (China), respectively. Rabbit pAbs directed against PR65α, PP2Ac, and p-PP2Ac were purchased from ABclonal (China). Mouse mAbs directed against PRRSV nsp4 and N protein have been described previously [18].

The HMGCR inhibitor Lovastatin and nuclear dye propidium iodide (red) were purchased from MedChemExpress (MCE, USA). The cholesterol dye filipin was purchased from Sigma-Aldrich (USA).

2.2. Plasmid construction

The eukaryotic expression plasmids (HA-tag) encoding PRRSV nonstructural proteins (nsps) [43] and the nsp4 protease mutants (H39A, D64A, and S118A) have been described previously [44]. PRRSV nsp4, nsp4 domain I (amino acids 1–80), nsp4 domain II (amino acids 60–156) and nsp4 domain III (amino acids 157–204) were generated with PCR amplification from pCAGGS-HA-nsp4 encoding full-length nsp4 and cloned into expression vector pEGFP-C1. The expression plasmids encoding Flag-tagged PR65α and PP2Ac were constructed from fragments amplified with PCR from the cDNA of PK-15^{CD163} cells, which were then cloned into the pCAGGS-Flag vector. All constructs were confirmed with DNA sequencing.

2.3. Cellular cholesterol content measurement

PAMs and PK-15^{CD163} cells were seeded into 6-well plates, and then infected with PRRSV at a multiplicity of infection (MOI) of 1.0 or transfected with nsp4, nsp4 domain I, nsp4 domain II, or nsp4 domain III for 12, 24, and 36 h. Next, the cells were harvested using 0.25% trypsin-EDTA. The concentrations of cholesterol in the collected cells were determined with a commercial cholesterol analysis kit (Amplex™ Red Cholesterol Assay Kit) manufactured by Thermo Fisher Scientific (USA). Similarly, the cholesterol content in PK-15^{CD163} cells pretreated with Lovastatin for 8 h and then mock-infected or infected with PRRSV (1.0 MOI) for 24 h was also analyzed.

2.4. Filipin staining

Cholesterol accumulation was assessed using filipin (Sigma-Aldrich, USA). PAMs and PK-15^{CD163} cells infected with PRRSV (MOI = 1.0) or transfected with nsp4 for 12, 24, and 36 h were fixed with 4% paraformaldehyde for 15 min, and then permeabilized with methanol for 10 min before the addition of filipin dye for 1 h at room temperature. The cells were washed with phosphate-buffered saline (PBS), and then incubated with the nuclear dye propidium iodide (MCE, USA) for 15 min. Fluorescent images were acquired with a confocal laser scanning microscope (Olympus Fluoviewer. 3.1, Japan).

2.5. Protein extraction and western blotting

Proteins were extracted with lysis buffer (Beyotime, China). The extracted proteins were separated with sodium dodecyl sulfate polyacrylamide gel electrophoresis (SDS-PAGE) and transferred to polyvinylidene difluoride (PVDF) membranes (Millipore, USA). After blocking with 5% (w/v) skim milk, the membranes were separately probed with the antibody against HMGCR, p-HMGCR, AMPK, p-AMPK, PP2Ac, p-PP2Ac, PR65α, PRRSV-N, PRRSV-nsp4, HA, Flag, GFP or

β-actin, and subsequent horseradish peroxidase-conjugated anti-mouse IgG or horseradish peroxidase-conjugated anti-rabbit IgG (Beyotime, China). The antibodies were diluted with PBS containing 0.1% Tween 20. The signals were visualized using Clarity Western ECL Substrate (Bio-Rad, USA) and band intensities were analyzed using the Image J2x software (Germany).

2.6. Coimmunoprecipitation assay

HEK-293T cells were co-transfected with expression plasmids encoding Flag-tagged PR65α/PP2Ac and HA-tagged nsp4, or expression plasmids encoding Flag-tagged PR65α/PP2Ac and EGFP-tagged nsp4/nsp4 domain I/nsp4 domain II/nsp4 domain III. At 36 h post transfection, the cells were collected and lysed by resuspension in 50 mM Tris–HCl (pH 8.0) containing 150 mM NaCl and 1% Triton X-100, 1% sodium deoxycholate, 0.1% SDS, 20 nM PMSF, and PhosSTOP phosphatase inhibitor (Sigma, USA). For immunoprecipitation, the lysates were incubated with the antibody against Flag, HA or GFP (MBL, Japan) for 12 h at 4 °C, and then precipitated with protein A/G agarose beads (Beyotime, China). After three washes with lysis buffer to remove non-adherent proteins, the captured proteins were analyzed by immunoblotting.

To further demonstrate the potential interactions between nsp4 and PR65α/PP2Ac under PRRSV infection, PK-15^{CD163} cells were infected with PRRSV (MOI = 1.0) for 36 h, then the cells were collected and lysed as described above, followed by the immunoprecipitation with nsp4-specific antibody and mouse normal IgG antibody, respectively.

2.7. Cytotoxicity analysis of Lovastatin

PK-15^{CD163} cells were treated with different concentrations (0, 2.5, 5, 10, 20 μM) of Lovastatin (MCE, USA) for 36 h, and then the number of nonviable cells was determined with the commercial CytoTox-ONE™ Homogeneous Membrane Integrity Assay, manufactured by Promega (USA).

2.8. RNA isolation and quantitative reverse transcription PCR (RT-qPCR)

The mRNA levels of IFN-β in PK-15^{CD163} cells transfected with nsp4 and its three truncations, or infected with PRRSV (1.0 MOI) for 24 h were analyzed. The IFN-β mRNA levels in PK-15^{CD163} cells pretreated with Lovastatin for 8 h and then transfected with nsp4 and its three truncations or infected with PRRSV (1.0 MOI) for 24 h were also analyzed. RNA was extracted with TRIzol Reagent (Invitrogen, USA), and then reverse transcribed into cDNA with the Transcriptor First Strand cDNA Synthesis Kit (Roche, Switzerland), according to the manufacturer's instructions. The quantitative PCR (qPCR) was performed using ABI 4367659Power SYBR Green Master Mix (USA) and ViiA™7 Real-Time PCR system (ABI, USA). The mRNA expression levels were normalized by β-actin. The following primers were used for qPCR: porcine IFN-β (F: 5′-GCTAACAAGTGCATCCTCCAAA 3′, R: 5′-AGCACATCATAGCTCATGGAAAGA-3′); porcine β-actin (F: 5′-TGAGAACAGCTGCATCCACTT-3′, R: 5′- CGAAGGCAGCTCGGAGTT-3′).

The virus RNA copies were also determined by RT-qPCR. PK-15^{CD163} cells pretreated with Lovastatin for 8 h were infected with PRRSV (1.0 MOI) for 24 h. RNA was isolated and reverse transcribed, then qPCR was performed as described above. Especially, the expression plasmid encoding HA-tagged nsp9 was used as a standard plasmid. The PRRSV nsp9-specific primers used for qPCR are as follows: (F: 5′-ACCCTAGGACCTGTGAAC-3′, R: 5′-GGCGAGTAACTTAGGAGATG-3′).

2.9. Detection of virus titer via plaque assay

PK-15^{CD163} cells were incubated with various concentrations of Lovastatin (2.5, 5, or 10 μM) for 8 h, and then infected with PRRSV (MOI = 1.0) for 24 h. The samples were collected through repeated freezing–thawing and centrifugation for virus titer determination. PK-15^{CD163} cells were cultured in six-well plates, chilled at 4 °C for 1 h, and the culture medium was replaced with serial 10-fold dilutions of samples. After incubation at 4 °C for another 2 h, the cells were washed with prechilled PBS, covered with overlay medium (DMEM containing 0.9% [w/v] low melting-point agarose), and incubated at 37 °C for a further ~72 h. The cells were stained with neutral red dye (0.05 mg/mL), and the number of plaques was counted to estimate the titer of PRRSV.

2.10. Statistical analysis

GraphPad Prism 5 (GraphPad Software) was used for all data analysis. Differences between groups were evaluated with a two-tailed unpaired *t*-test, and involved three groups or more were evaluated with ANOVA test, and were considered statistically significant when the *p* value was less than 0.05.

3. Results

3.1. PRRSV infection upregulates cellular cholesterol

To investigate the effects of PRRSV infection on cellular cholesterol levels, PAMs and PK-15^{CD163} cells were infected with PRRSV (MOI = 1.0). The cellular cholesterol contents were determined with the Amplex™ Red Cholesterol Assay Kit at 12, 24, and 36 h post infection (hpi). The levels of cellular cholesterol were significantly upregulated in both PAMs and PK-15^{CD163} cells as PRRSV infection progressed (Fig. 1A and B). To optically quantify the accumulation of intracellular cholesterol, cholesterol was classically stained with filipin to visualize the cholesterol fluctuations in PAMs and PK-15^{CD163} cells infected with PRRSV (MOI = 1.0). As shown in Fig. 1C and D, PRRSV infection increased the intracellular cholesterol concentration.

3.2. PRRSV infection upregulates HMGCR activity through the PP2A pathway

Cholesterol synthesis is a process catalyzed by various enzymes, and HMGCR is the key rate-limiting enzyme [27]. It has been demonstrated that HMGCR phosphorylation is associated with AMPK and PP2A, insofar as PP2A dephosphorylates HMGCR to activate it and AMPK phosphorylates HMGCR to reduce its activity (Fig. 2A) [36]. To investigate whether PRRSV infection upregulates the activity of HMGCR, the levels of HMGCR phosphorylated at Ser-872 (inactive form) were determined in PAMs and PK-15^{CD163} cells infected with PRRSV (MOI = 1.0) at different time points (12, 24, and 36 hpi) with western blotting. Compared with the control cells, the ratio of phosphorylated HMGCR to total HMGCR (p-HMGCR/HMGCR) was significantly lower in the cells infected with PRRSV than in the uninfected cells, indicating enhanced HMGCR activity, as shown in Fig. 2B. To assess the contribution of AMPK to HMGCR activation during PRRSV infection, the protein levels of AMPK phosphorylated at Thr172 and total AMPK were measured in PAMs and PK-15^{CD163} cells infected with PRRSV (MOI = 1.0). An increase in AMPK phosphorylation (active form) was observed in PRRSV-infected cells at 24 and 36 hpi (Fig. 2C). Theoretically, increased AMPK phosphorylation should reduce the activity of HMGCR, which is inconsistent with the finding that PRRSV infection upregulates HMGCR activity. Therefore, AMPK signaling may not be involved in the PRRSV-mediated activation of HMGCR. We then analyzed the change in the level of phosphorylated PP2A (p-PP2Ac; inactive form) in response to PRRSV infection in PAMs and PK-15^{CD163} cells at 12, 24, and 36 hpi. The results presented in Fig. 2D showed that the level of p-PP2Ac decreased significantly after PRRSV infection, which corresponded to the fluctuation in p-HMGCR. The specificities of antibodies against p-HMGCR, p-AMPK and p-PP2Ac were demonstrated (Supplementary Fig. 1). Based on these results, we concluded that PRRSV upregulated HMGCR activity mainly through PP2A, and not through AMPK.

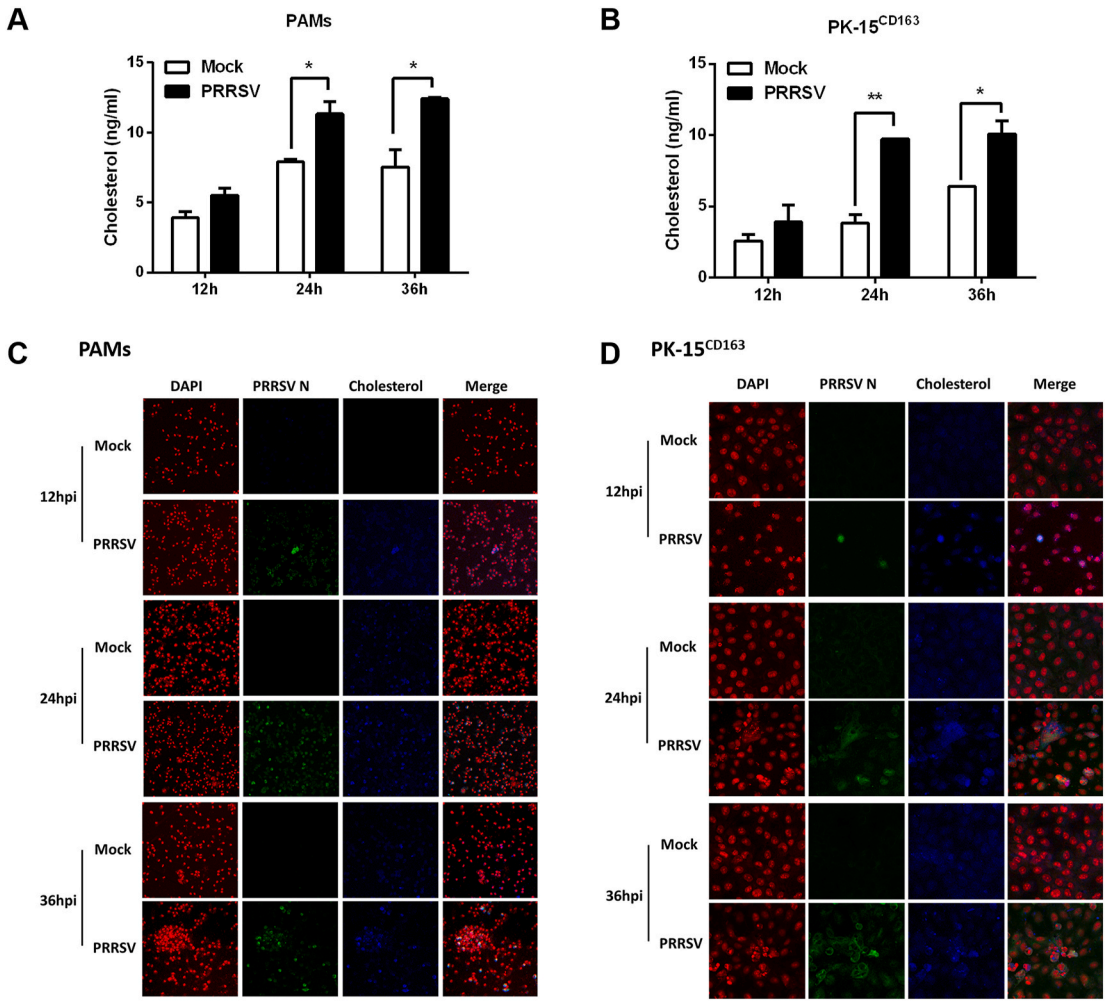

Fig. 1. Cellular cholesterol is upregulated in PRRSV-infected cells. PAMs or PK-15^{CD163} cells were infected with PRRSV (MOI = 1.0). At the indicated time points after infection, the cells were harvested for the quantitation of cholesterol with the Amplex™ Red Cholesterol Assay Kit **(A, B)**, or the cells were fixed to detect the cholesterol content with the cholesterol dye filipin (blue) **(C, D)**. The nuclei were counterstained with propidium iodide (red). Fluorescent images were acquired with a confocal laser scanning microscope. The presented results represent the means and standard deviations of data from three independent experiments (*p ≤ 0.05; **p ≤ 0.01). (For interpretation of the references to colour in this figure legend, the reader is referred to the Web version of this article.)

3.3. PRRSV nsp4 upregulates cellular cholesterol levels independently of its protease activity

To screen which protein encoded by PRRSV is involved in the activation of HMGCR, we then transfected PK-15^{CD163} cells with expression vectors encoding hemagglutinin (HA)-tagged PRRSV proteins (except nsp2TF, nsp2N, nsp6, nsp8 and ORF5a) and used western blotting to detect the expression of p-HMGCR. As shown in Fig. 3A, PRRSV nsp4 significantly impeded HMGCR phosphorylation, whereas the other viral proteins had little effect. To confirm this result, PK-15^{CD163} cells were transfected with different amounts of plasmid encoding HA-tagged nsp4, and the expression levels of p-HMGCR and p-PP2Ac were assessed with western blotting at 36 h post transfection. The results showed that PRRSV nsp4 activated HMGCR activity in a dose-dependent manner, and a similar pattern of p-PP2Ac expression was also observed (Fig. 3B).

It is well known that PRRSV nsp4 is a 3C-like protease (3CLP) responsible for most of the cleavages of viral polyproteins. His39 (H39), Asp64 (D64), and Ser118 (S118) of nsp4 are essential for its 3CLP activity, and any mutation at these three sites abrogates its protease activity [45]. To examine whether the 3CLP activity of nsp4 participates in the process by which nsp4 regulates PP2A activity, we measured the PP2A phosphorylation levels in PK-15^{CD163} cells transfected with constructs expressing nsp4 or one of three mutant forms (H39A, D64A, or S118A). As shown in Fig. 3C, there existed no difference in phosphorylated PP2A levels, indicating that nsp4 regulating PP2A phosphorylation was not associated with its 3CLP activity.

We then examined whether PRRSV nsp4 is involved in the PRRSV-induced upregulation of cholesterol. The cholesterol levels in PK-15^{CD163} cells transfected with plasmid expressing HA-tagged nsp4 were detected. The levels of cholesterol in the PK-15^{CD163} cells expressing nsp4 were significantly higher than those in the control cells (Fig. 3D and E). Based on these results, we concluded that PRRSV nsp4 modulated HMGCR activity to upregulate cellular cholesterol levels (mainly through PP2A), independently of its protease activity.

3.4. PRRSV nsp4 interacts with PP2A

PP2A is composed of a 65-kDa structural subunit (PR65α; A subunit), a regulatory B subunit, and a 35-kDa catalytic subunit (PP2Ac; C subunit), and the core enzyme of PP2A consists of PR65α and PP2Ac [46] (Fig. 4A). To further investigate the mechanism by which PRRSV nsp4 activated PP2A, we studied the interactions between PR65α or PP2Ac and PRRSV nsp4. We founded that nsp4 interacted with both PR65α and PP2Ac (Fig. 4B). In the reverse Co-IP experiments, nsp4 and PR65α or PP2Ac proteins were also efficiently coimmunoprecipitated with an anti-HA antibody (Fig. 4C). We also investigated whether the association

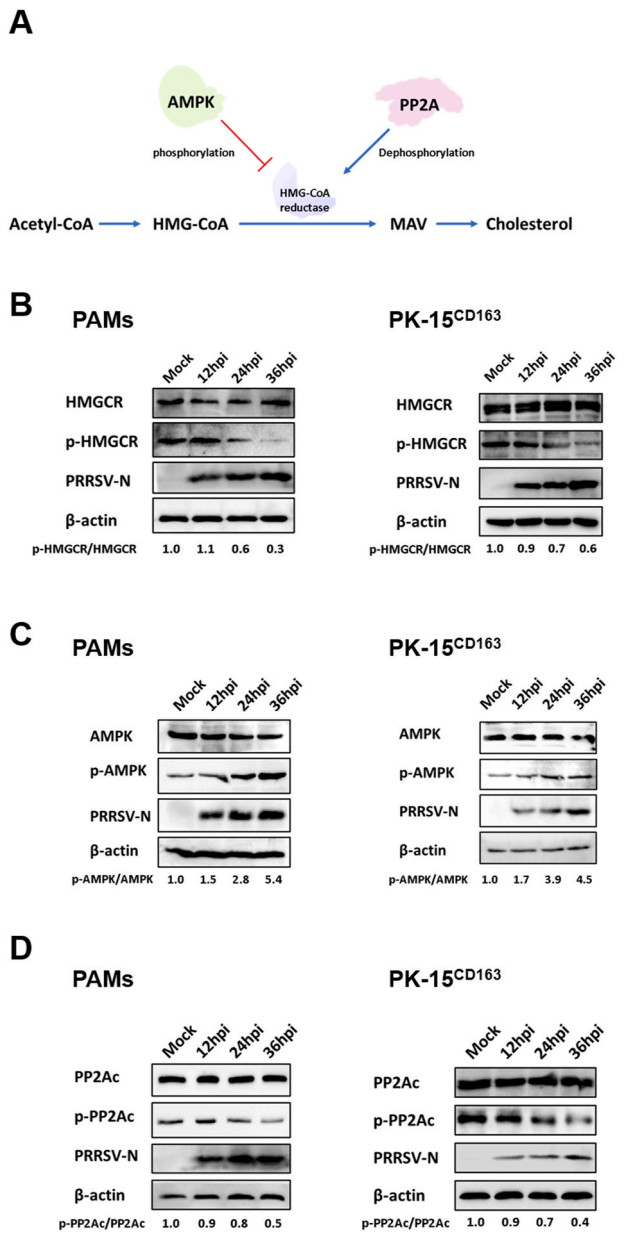

Fig. 2. PRRSV infection activates the PP2A–HMGCR pathway. (A) Model of cholesterol synthesis via the AMPK–HMGCR and PP2A–HMGCR pathways. Level of p-HMGCR (inactive form) was enhanced by AMPK, resulting in the downregulation of cholesterol synthesis, but reduced by PP2A, resulting in the upregulation of cholesterol synthesis. **(B–D)** PAMs or PK-15^{CD163} cells infected with PRRSV (MOI = 1.0) were harvested at 12, 24, and 36 hpi. The expression levels of total HMGCR and phosphorylated HMGCR (p-HMGCR) **(B)**, total AMPK and p-AMPK **(C)**, or total PP2Ac and p-PP2Ac **(D)** were analyzed with western blotting. PRRSV infection was verified by detecting the expression of viral N protein with anti-N antibody. The β-actin was used as the protein loading control.

between nsp4 and the PR65α or PP2Ac proteins occurs during PRRSV infection. The results showed that nsp4 interacted with the endogenous PR65α and PP2Ac proteins in PRRSV-infected PK-15^{CD163} cells (Fig. 4D).

3.5. PRRSV nsp4 domain I interacts with PP2A

Having confirmed the interaction between nsp4 and the PR65α and PP2Ac subunits of PP2A, we mapped the region(s) of nsp4 that interacted with PP2A. Based on previous studies and the structure of PRRSV nsp4, three truncations containing amino acids 1–80 (domain I), 60–156 (domain II), or 157–204 (domain III) were generated and fused to the enhanced green fluorescent protein (EGFP) gene [45] (Fig. 5A). HEK-293T cells co-transfected with nsp4/domain I/domain II/domain III and PR65α/PP2Ac were lysed and then immunoprecipitated with an anti-Flag antibody. Domain I, but not domain II or III, of nsp4 interacted with PR65α and PP2Ac (Fig. 5B and D), indicating that PP2A is specifically targeted by domain I of nsp4. In a reverse Co-IP experiment, an anti-GFP antibody efficiently coimmunoprecipitated nsp4 domain I and PR65α or PP2Ac (Fig. 5C and E). These results indicated that domain I of nsp4 interacted with both subunits of PP2A: PR65α and PP2Ac.

3.6. Lovastatin abolishes the inhibition of IFN-β mediated by nsp4 domain I

To verify whether nsp4 domain I is involved in the regulation of cholesterol, the cholesterol content of PK-15^{CD163} cells transfected with nsp4 and its three truncations were analyzed. The results showed that nsp4 and domain I up-regulated intracellular cholesterol, while nsp4 domain II and nsp4 domain III had a weak effect (Fig. 6A). A previous study reported that the restriction of cholesterol synthesis spontaneously induces the IFN-I response [40]. Because PRRSV nsp4 is a well-known IFN-I antagonist and also increases cellular cholesterol levels, we speculated that PRRSV nsp4 may inhibit IFN-β production by upregulating cellular HMGCR activity and cholesterol levels. To test this hypothesis, the antagonistic activities of nsp4 and its three truncations against IFN-β were analyzed. Quantitative reverse transcription PCR (RT-qPCR) showed that nsp4 domains I and II reduced the IFN-β mRNA levels induced by Sendai virus (Fig. 6B). Because nsp4 domain I significantly up-regulated intracellular cholesterol, suggesting the possibility that cholesterol was involved in the antagonism of IFN-β production by PRRSV nsp4 domain I. Then we used Lovastatin, an HMGCR inhibitor, to reduce cellular cholesterol and then detected type I IFN levels. Only low cytotoxicity of Lovastatin was detected in PK-15^{CD163} cells at the concentrations ≤10 μM (Fig. 6C). We also measured the cholesterol levels in PK-15^{CD163} cells after treatment with Lovastatin, and the results showed that 10 μM Lovastatin effectively reduced cellular cholesterol to a very low level (Fig. 6D). The antagonistic activity of IFN-β by PRRSV nsp4 in PK-15^{CD163} cells pretreated with Lovastatin was detected. The results showed that Lovastatin pretreatment impaired the inhibitory effect of nsp4 on IFN-β production to some degree. It almost completely abolished the inhibitory effect of nsp4 domain I, but had no effect on the inhibition of IFN-β production mediated by nsp4 domain II (Fig. 6E). These results suggested that the inhibition of IFN-β mediated by PRRSV nsp4 domain I depended upon the upregulation of cellular HMGCR activity and cholesterol levels.

3.7. Lovastatin inhibits PRRSV proliferation

To measure whether the change of cholesterol during PRRSV infection is synchronized with IFN-β, the cholesterol and IFN-β levels in PK-15^{CD163} cells pretreated with Lovastatin during PRRSV infection were analyzed. The results showed that Lovastatin inhibited the production of cholesterol induced by PRRSV infection (Fig. 7A) and weakened the inhibitory effect of PRRSV on IFN-β (Fig. 7B). These data displayed that PRRSV could inhibit the production of IFN-β by targeting cholesterol. Considering Lovastatin treatment partly eliminated the inhibitory effects of PRRSV on type I IFN production, we investigated whether Lovastatin treatment affects PRRSV multiplication. The results indicated that Lovastatin significantly suppressed PRRSV proliferation in a dose-dependent manner, as demonstrated by the viral titers (Fig. 7C), viral genome copies (Fig. 7D) and viral protein expression levels (Fig. 7E).

4. Discussion

Growing evidences indicate an intimate relationship between intracellular pathogens and the host's cholesterol metabolism. Cholesterol is

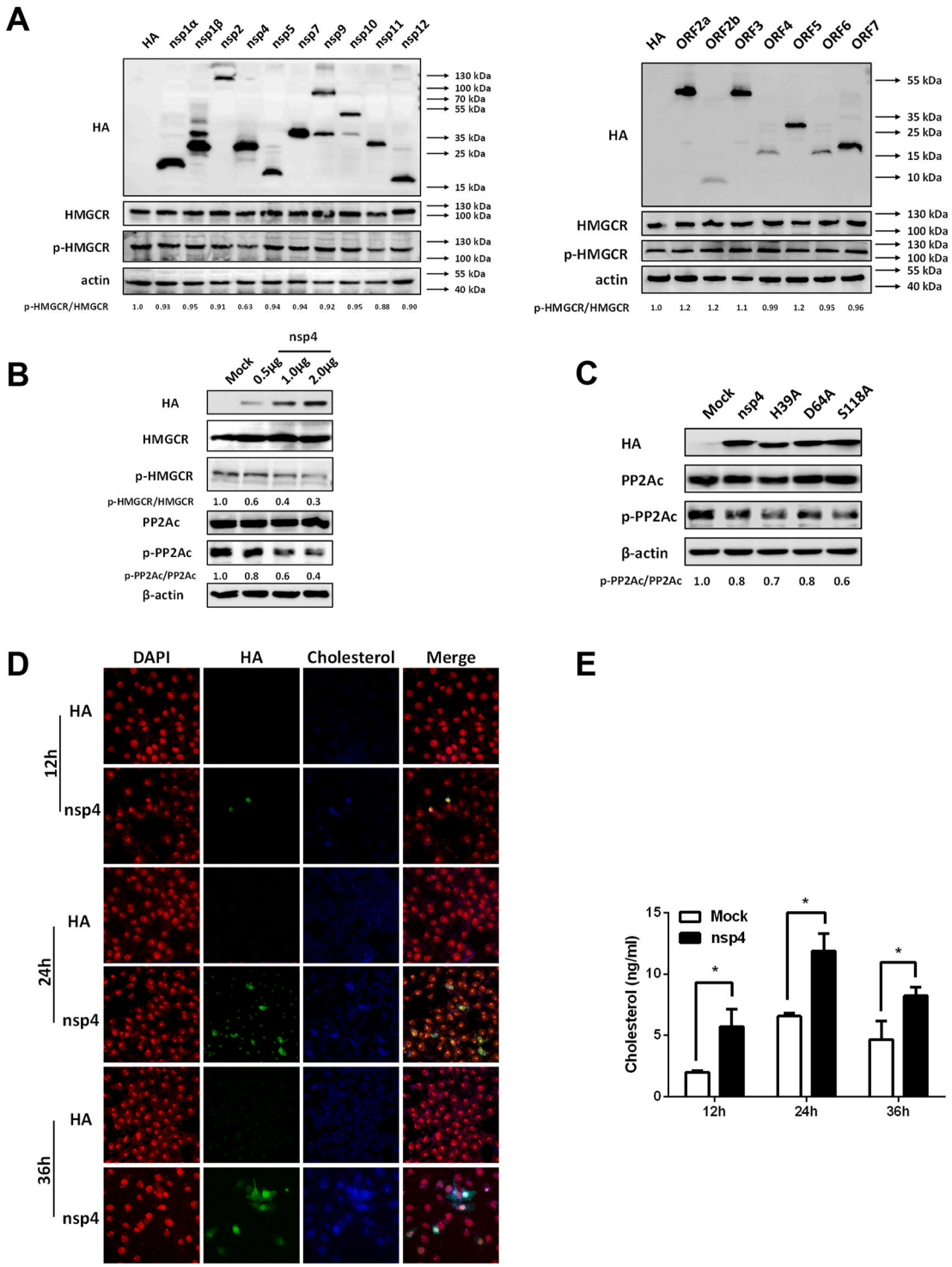

Fig. 3. PRRSV nsp4 plays a major role in upregulating cellular cholesterol independently of its protease activity. (A) PK-15^{CD163} cells were transfected with expression vectors encoding HA-tagged PRRSV-encoded proteins. The levels of HMGCR and p-HMGCR were determined with western blotting at 36 h post transfection. **(B)** PK-15^{CD163} cells were transfected with different doses of plasmids encoding HA-tagged PRRSV nsp4. The cell lysates were harvested and the expression levels of HMGCR, p-HMGCR, PP2Ac and p-PP2Ac were analyzed with western blotting. **(C)** PK-15^{CD163} cells were transfected with expression vectors encoding HA-tagged nsp4 or nsp4 mutant (H39A, D64A, or S118A). At 36 h post transfection, the cells were harvested to analyze PP2Ac and p-PP2Ac levels with western blotting. **(D)** PK-15^{CD163} cells were transfected with an expression vector encoding HA-tagged nsp4. At 12, 24, and 36 h post transfection, cells were fixed to determine the cholesterol content using the cholesterol dye filipin (blue). The nuclei were counterstained with propidium iodide (red). Fluorescent images were acquired with a confocal laser scanning microscope. **(E)** PK-15^{CD163} cells were transfected with an expression vector encoding HA-tagged nsp4. The cells were harvested for the quantitation of cholesterol with the Amplex™ Red Cholesterol Assay Kit at 12, 24, and 36 h post transfection. The results presented are the means and standard deviations of data from three independent experiments (*$p \leq 0.05$). (For interpretation of the references to colour in this figure legend, the reader is referred to the Web version of this article.)

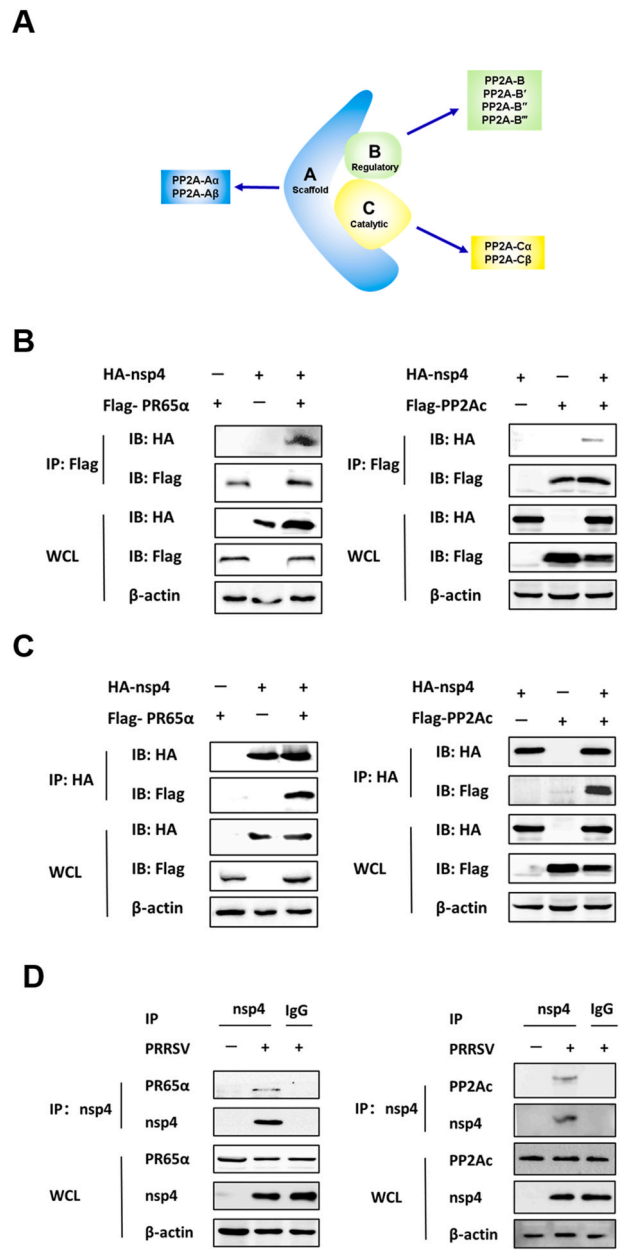

Fig. 4. PRRSV nsp4 interacts with PP2A. (A) PP2A consists of three subunits, including a structural subunit (scaffolding subunit; A subunit, PR65α), a regulatory subunit (B subunit), and a catalytic subunit (PP2Ac, C subunit). **(B, C)** HEK-293T cells were cotransfected with expression vector encoding Flag-tagged PR65α or PP2Ac and vector encoding HA-tagged PRRSV nsp4. The cells were lysed at 36 h post transfection and immunoprecipitated with anti-Flag **(B)** or anti-HA **(C)** antibody. Whole-cell lysates (WCLs) and immunoprecipitation (IP) complexes were analyzed with immunoblotting using anti-Flag, anti-HA, or anti-β-actin antibody. **(D)** PK-15^{CD163} cells were infected with PRRSV (MOI = 1.0). The cells were lysed at 36 hpi and immunoprecipitated with anti-nsp4 antibody. WCLs and IP complexes were analyzed with immunoblotting using anti-nsp4, anti-PR65α, anti-PP2Ac, or anti-β-actin antibody.

essential for the entry, replication complex (RC) formation, assembly, and egress of many viruses, especially the enveloped RNA viruses. Cholesterol depletion studies using MβCD have suggested that membrane cholesterol is required for infections by such viruses as Human respiratory syncytial virus (RSV) [47], Porcine delta coronavirus (PDCoV) [48], Foot-and-mouth disease virus (FMDV) [49], Caprine parainfluenza virus type 3 (CPIV3) [50], Porcine rotavirus (PRoV) [51], Caprine herpesvirus type 1 (CpHV.1) [52], Newcastle disease virus (NDV) [53], and Hepatitis C virus (HCV) [54]. Therefore, many viruses modulate the cholesterol metabolism of cells to allow viral replication. Previous studies have shown that viruses mainly regulate intracellular cholesterol levels by reducing cholesterol efflux or promoting the *de novo* synthesis of cholesterol. For example, DENV increases cholesterol synthesis by increasing HMGCR activity through the reduction of AMPK phosphorylation [36], and prevents cholesterol efflux by reducing the expression of low-density lipoprotein receptor-related protein 1 (LRP1), thus increasing intracellular cholesterol level [55]. Previously, our group reported that MβCD inhibits the release and entry processes of PRRSV, implying that cholesterol is essential for PRRSV infection [56]. However, the effect of PRRSV infection on the cellular cholesterol content and the molecular mechanisms involved had not been studied. In this study, we demonstrated that the increased *de novo* synthesis of cholesterol during PRRSV infection was mediated by the upregulation of HMGCR activity via the dephosphorylation of PP2A.

The increase in HMGCR activity stimulates the cholesterol synthesis required for PRRSV infection. This was confirmed by the treatment of infected cells with Lovastatin, an HMGCR inhibitor, which inhibited the proliferation of PRRSV. However, the specific stage of PRRSV infection targeted by Lovastatin has not been identified. Because PRRSV is an enveloped virus, the invasion and release stages of PRRSV infection require the participation of the cytomembrane. The reduction of cholesterol, a key component of membrane lipids, disrupts the cytomembrane lipid microdomains involved in the invasion and release of PRRSV. The consumption of cholesterol may also affect the binding of PRRSV to its core receptor, CD163, a membrane protein, when the membrane fluidity is disturbed, thereby affecting the PRRSV invasion process mediated by CD163. Therefore, we speculate that Lovastatin, which reduces the level of cholesterol and destroys the cytomembrane structure, antagonizes PRRSV infection by targeting its invasion and release processes. Our previous studies have shown that the cholesterol chelator, MβCD, inhibits the invasion and release of PRRSV during infection, and that 25HC, a negative regulator of cholesterol biosynthesis [57,58], prevents PRRSV infection by inhibiting PRRSV invasion [59–61]. Interestingly, the synthesis of PRRSV RNA depends on a remodeled intracellular membrane structure, which acts as a platform for the efficient and correct assembly of RTC [62,63]. This suggests that Lovastatin is also likely to interfere with the replication of the PRRSV genomic RNA. The mechanism(s) by which Lovastatin restricts PRRSV infection requires further research.

As well as its roles in various intracellular physiological processes, PP2A, a type 2 protein phosphatase, is utilized by many viruses in distinct ways to facilitate viral infection. Several viral proteins have been shown to interact directly with PP2A. For example, the interaction of Human T-cell leukemia virus type-1 (HTLV-1) integrase and the PP2A B56γ subunit leads to the formation of a higher-order nucleoprotein assembly (intasome) that mediates HTLV-1 integration [64]. The small T antigen of Simian virus 40 (SV40) interacts with the A subunit of PP2A, downregulating PP2A activity, and resulting in cell transformation and tumorigenesis [65]. The Human papilloma virus E7 protein binds to both A and C subunits of PP2A, inhibiting the dephosphorylation of PP2A and maintaining the PI3K–AKT transforming pathway [66]. The Ebola virus nucleoprotein recruits the host PP2A-B56 phosphatase to activate viral transcription factor VP30, promoting viral replication [67]. In plants, the glutamate at position 142 of the protein phosphatase PP2C and the serine residue at position 89 of the PYL protein form a hydrogen bond, which affects the binding of PP2C to Mg^{2+} and Mn^{2+}, thereby inhibiting the enzyme activity of PP2C. In addition, the serine at position 89 of PYL2 can also bind to the glycine on the active site of PP2C to form a hydrogen bond, preventing the substrate protein from entering the catalytic active center of PP2C, thereby directly inhibiting the activity of PP2C phosphatase [68]. In this study, PRRSV nsp4 was shown to interact with the A and C subunits of PP2A, thereby reducing the phosphorylation of PP2Ac. However, how PRRSV nsp4 affects the activity of PP2A still needs further research. PP2A possesses three

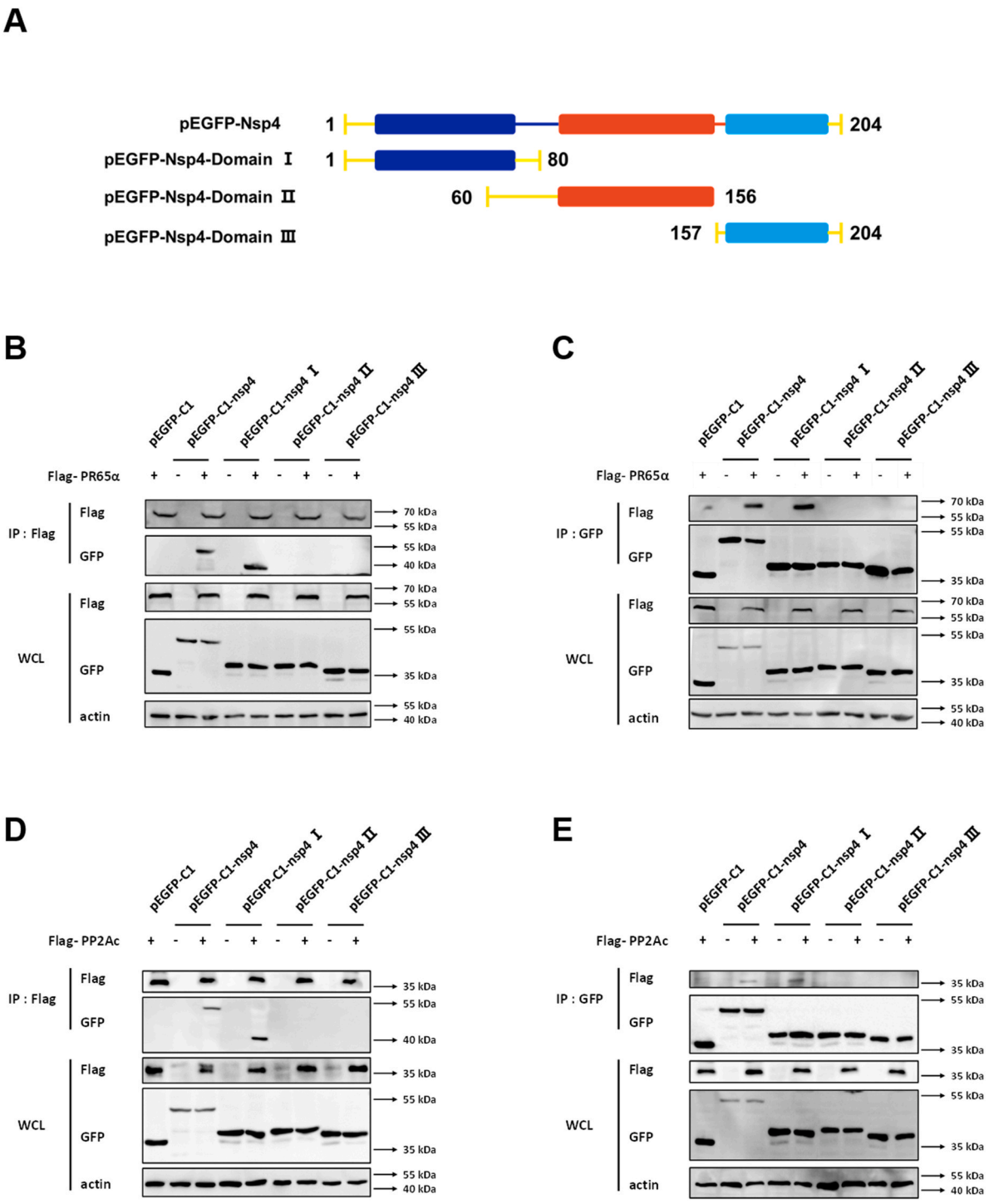

Fig. 5. PRRSV nsp4 domain I (amino acids 1–80) interacts with the structural subunit (PR65α) and catalytic subunit (PP2Ac) of PP2A. (A) Schematic diagram of nsp4 truncations. **(B–E)** HEK-293T cells were co-transfected with expression vectors encoding Flag-tagged PR65α or PP2Ac and EGFP-tagged nsp4, nsp4 domain I, nsp4 domain II, or nsp4 domain III. The cells were lysed at 36 h post transfection and immunoprecipitated with an anti-Flag antibody **(B, D)** or an anti-GFP antibody **(C, E)**. The WCLs and IP complexes were analyzed with immunoblotting using anti-Flag, anti-EGFP, or anti-β-actin antibody.

phosphorylation sites (S303, T268, and S314) in A subunit, and two phosphorylation sites (T304 and Y307) in C subunit [69,70], with the phosphorylation at Y307 widely regarded as a marker of PP2A inactivation. Thus, the binding site of nsp4 may overlap with the phosphorylation sites of PP2A, which may affect the binding of PP2A to metal ions [71–73], or prevent the substrate protein from entering the active center of PP2A, and then inhibit PP2A phosphorylation. Numerous viruses also disturb various host signaling pathways through PP2A. The HCV-induced upregulated expression of PP2Ac contributes to hepatocarcinogenesis via the dysregulation of epigenetic histone modifications [74]. The HBV X protein impairs IFN-α signaling by upregulating PP2A expression [75]. Cellular SP1 and NF-κB, two transcription factors regulated by PP2A signaling [76,77], are essential modulators of many viruses, including Human immunodeficiency virus 1 (HIV-1), Cytomegalovirus, Herpes simplex type 1, Epstein-Barr virus, and Papillomavirus [78]. Thus, PP2A offers a potent therapeutic target for many

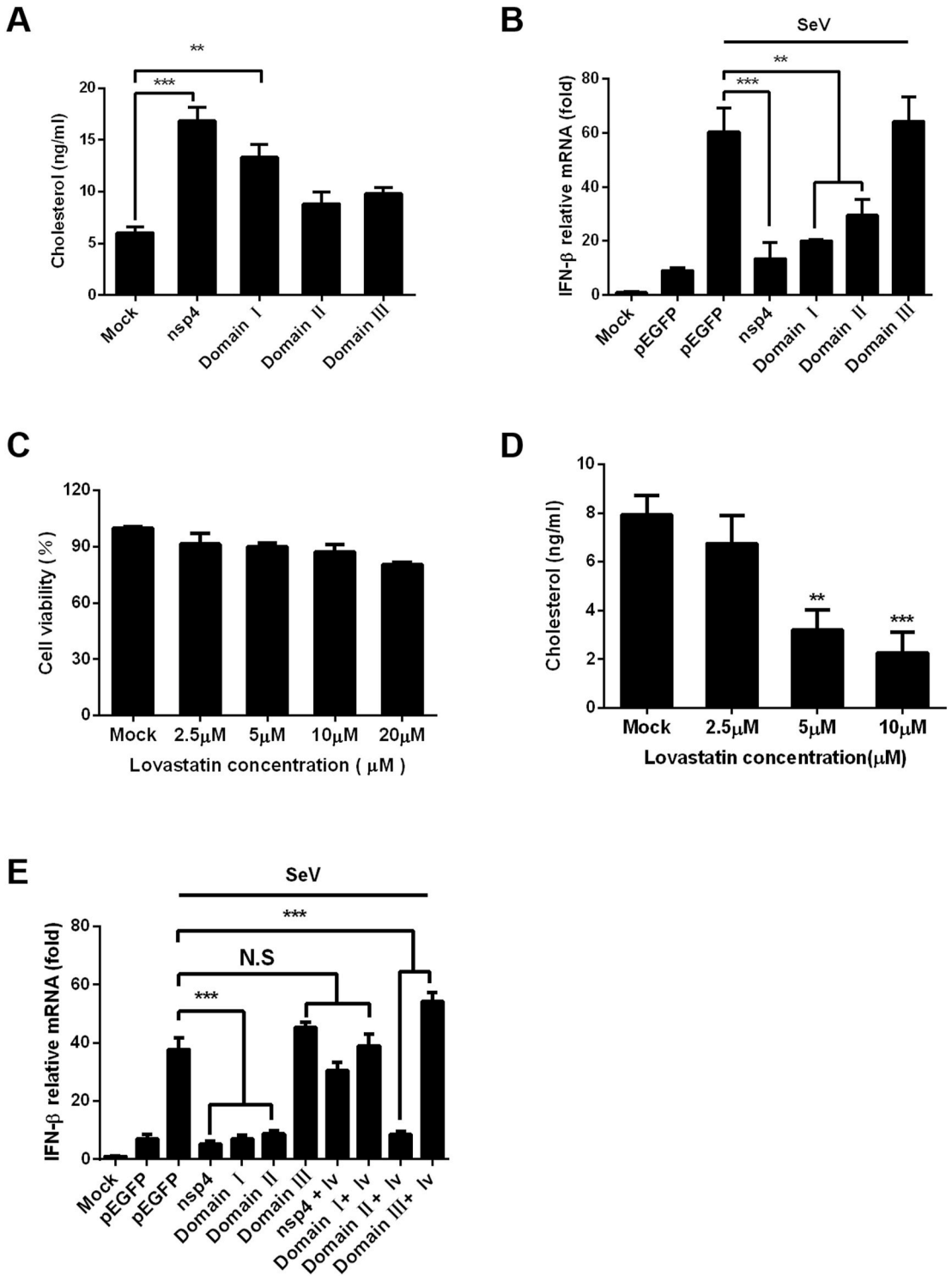

Fig. 6. Lovastatin eliminates the IFN-β inhibitory effect mediated by PRRSV nsp4 domain I. (A) PK-15^{CD163} cells were transfected with expression vector encoding EGFP-tagged nsp4 or its truncation (domain I, domain II, or domain III), and then the cellular cholesterol levels were determined with the Amplex™ Red Cholesterol Assay Kit. **(B)** PK-15^{CD163} cells were transfected with expression vector encoding EGFP-tagged nsp4 or its truncation (domain I, domain II, or domain III), and then stimulated with Sendai virus (SeV) for 12 h. The total cellular RNAs were extracted to determine the IFN-β mRNA levels with RT–qPCR. **(C)** PK-15^{CD163} cells were incubated with the indicated concentrations of Lovastatin for 36 h and cytotoxicity was detected with the CytoTox-ONE™ Homogeneous Membrane Integrity Assay. **(D)** PK-15^{CD163} cells were incubated with various concentrations (2.5, 5, or 10 μM) of Lovastatin, and the cellular cholesterol levels were then determined with the Amplex™ Red Cholesterol Assay Kit. **(E)** PK-15^{CD163} cells were pretreated with Lovastatin (Lv; 10 μM) for 8 h, and then transfected with an expression vector encoding EGFP-tagged nsp4 or its truncation (domain I, domain II, or domain III), followed by stimulation with SeV for 12 h. The total cellular RNAs were extracted to determine the IFN-β mRNA levels with RT–qPCR. The results presented are ANOVA of data from three independent experiments (**$p \leq 0.01$; ***$p \leq 0.001$).

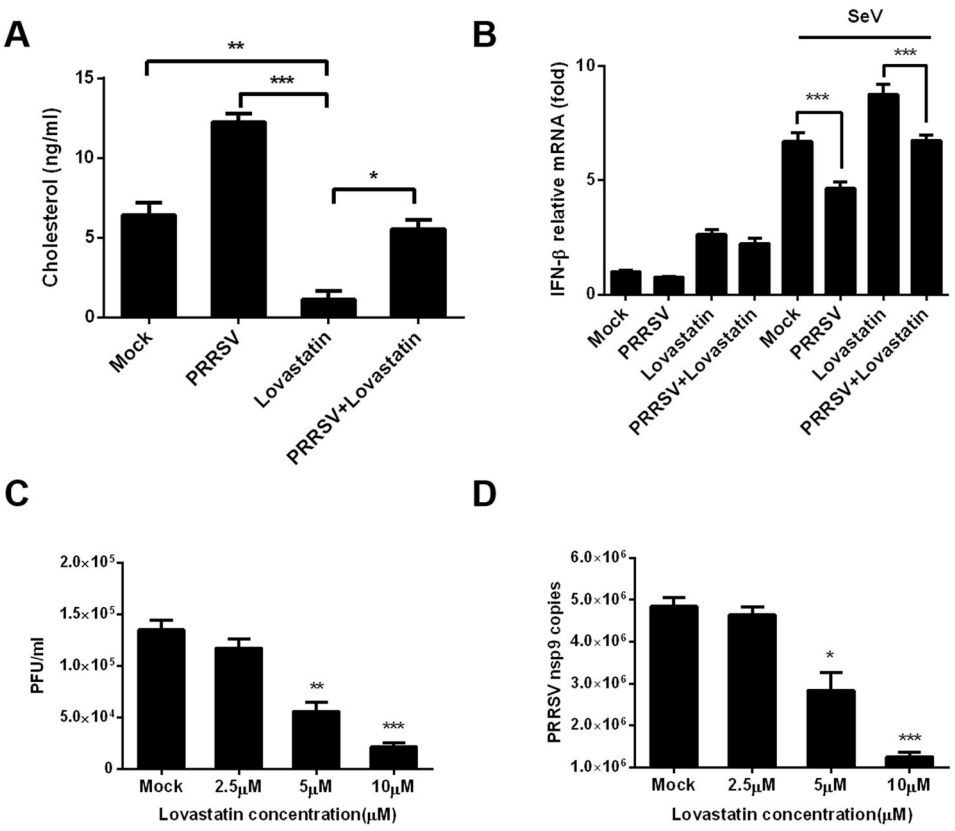

Fig. 7. Lovastatin inhibits PRRSV infection. (A) PK-15^{CD163} cells were pretreated with 10 μM Lovastatin for 8 h before PRRSV infection (MOI = 1.0), and then the cellular cholesterol levels were determined with the Amplex™ Red Cholesterol Assay Kit. **(B)** PK-15^{CD163} cells were pretreated with 10 μM Lovastatin for 8 h before PRRSV infection (MOI = 1.0), and then stimulated with SeV for 12 h. The total cellular RNAs were extracted to determine the IFN-β mRNA levels with RT–qPCR. **(C–E)** PK-15^{CD163} cells were pretreated with different concentrations of Lovastatin for 8 h before PRRSV infection (MOI = 1.0). Infected cells were cultured in the presence of the indicated concentrations of Lovastatin and harvested at 24 hpi for a plaque assay **(C)**, RT–qPCR **(D),** and western blotting **(E)**. The results presented are ANOVA of data from three independent experiments (*$p \leq 0.05$; **$p \leq 0.01$; ***$p \leq 0.001$).

viruses in the future.

The IFN response constitutes the first line of defense in the early control of viral infection. Consequently, viruses have developed a variety of defensive strategies to inhibit IFN production. PRRSV nsp4, a 3CLP responsible for processing most PRRSV nonstructural proteins, plays an important role in subverting the host's innate immune response. Previous studies have shown that the 3CLP activity of PRRSV nsp4 not only cleaves IFN-β promoter stimulator 1 (IPS-1) [17] and kinase NF-κB essential modulator (NEMO) [44], two key adapter molecules in the IFN-I synthesis pathway, but also interferon-stimulated genes (ISGs) such as zinc finger antiviral protein (ZAP) [19] and decapping mRNA 1A (DCP1A) [18], to dampen the host's antiviral innate immune responses. PRRSV nsp4 also induces the proteolytic cleavage of the mitochondrial inner membrane protein cytochrome *c*1 (CYC1) and the cleavage of the N-terminal fragment of CYC1 results in apoptotic cell death [79]. PRRSV nsp4 also facilitates the cleavage of procaspase 9 by activating B-cell lymphoma 2 (BCL2) interacting mediator of cell death and induces the degradation of B-cell lymphoma-extra-large (BCL-XL), an anti-apoptotic protein [80]. Thus, PRRSV nsp4 is a multifunctional protein. In the present study, we observed that nsp4 increased the activity of HMGCR to upregulate the production of cholesterol in a protease activity-independent manner, which subsequently decreased the levels of type I IFN (IFN-I). This is a novel feature of PRRSV nsp4, and extends our knowledge of its functions. Interestingly, both domain I and domain II of nsp4 exhibited inhibitory effects on IFN-I production, while only domain I significantly promoted cholesterol synthesis, suggesting that nsp4 domain II might suppress IFN-I through a cholesterol-independent mechanism, such as usage of its 3CLP activity. Previous study reveals that the PRRSV nsp4 truncation lacking domain II represses IFN-I response, and the inhibitory effect is independent of the 3CLP activity of nsp4 [15]. However, as described above, the 3CLP activity is also implicated in the nsp4-mediated reduction of IFN-I production, suggesting that nsp4 domain II, but not domain I and domain III, may exert inhibitory effects on IFN-I response depending on the protease activity of nsp4, which is coincident with our hypothesis.

In summary, we have shown that PRRSV infection reduces PP2A phosphorylation to activate HMGCR, resulting in an increase in cellular cholesterol, and that the viral protease nsp4 plays an important role in this process. We have also demonstrated that PRRSV nsp4 inhibits IFN-I production by regulating the cellular cholesterol metabolism, independently its protease activity. This is a novel mechanism, differing from the

previously known role of PRRSV nsp4 in proteolytically cleaving the host's antiviral innate immune molecules. These findings highlight the complexity of the strategies used by PRRSV to evade its host's innate immune response.

Funding

This work is supported by the National Natural Science Foundation of China (32130103, 32002279, 31490602) and the National Basic Research Program (973) of China (2014CB542700).

Declaration of competing interest

All the authors declare that there are no conflicts of interest.

Acknowledgments

We would like to thank Dr. Enmin Zhou for providing PK-15^{CD163} cells.

Appendix A. Supplementary data

Supplementary data to this article can be found online at https://doi.org/10.1016/j.redox.2021.102207.

Abbreviations

AEBSF	4-(2-aminoethyl) benzene sulfonyl fluoride
AMPK	Adenosine 5-monophosphate-activated protein kinase
BCL-XL	B-cell lymphoma-extra-large
BLC2	B-cell lymphoma 2
CH25H	Cholesterol-25-hydroxylase
CYC1	Cytochrome *c*1
DCP1A	Decapping mRNA 1A
HMGCR	3-hydroxy-3-methylglutaryl coenzyme A reductase
IFN	Interferon
IPS-1	IFN-β promoter stimulator 1
LRP1	Low-density lipoprotein receptor-related protein 1
MβCD	Methyl-β-cyclodextrin
NEMO	NF-κB essential modulator
ORFs	Open reading frames
PP2A	Protein phosphatase 2
PRRSV	Porcine reproductive and respiratory syndrome virus
RCs	Replication complexes
SLA- I	Swine leukocyte antigen class I
ZAP	Zinc finger antiviral protein
3CLP	3C-like protease
25HC	25-hydroxycholesterol

References

[1] G. Wensvoort, C. Terpstra, J.M. Pol, et al., Mystery swine disease in The Netherlands: the isolation of Lelystad virus, Vet. Q. 13 (3) (1991) 121–130.
[2] J.K. Lunney, Y. Fang, A. Ladinig, et al., Porcine reproductive and respiratory syndrome virus (PRRSV): pathogenesis and interaction with the immune system, Annu. Rev. Anim. Biosci. 4 (2016) 129–154.
[3] M.A. Kappes, K.S. Faaberg, PRRSV structure, replication and recombination: origin of phenotype and genotype diversity, Virology 479–480 (2015) 475–486.
[4] J. Shen, X. Yan, J. Dong, et al., Complete genome sequence of a novel deletion porcine reproductive and respiratory syndrome virus strain, Genome Announc. 1 (4) (2013) e00486-13.
[5] E.J. Snijder, M. Kikkert, Y. Fang, Arterivirus molecular biology and pathogenesis, J. Gen. Virol. 94 (Pt 10) (2013) 2141–2163.
[6] D. Cavanagh, Nidovirales: a new order comprising Coronaviridae and Arteriviridae, Arch. Virol. 142 (3) (1997) 629–633.
[7] Y. Li, A. Tas, E.J. Snijder, et al., Identification of porcine reproductive and respiratory syndrome virus ORF1a-encoded non-structural proteins in virus-infected cells, J. Gen. Virol. 93 (Pt 4) (2012) 829–839.
[8] Y. Li, A. Tas, Z. Sun, et al., Proteolytic processing of the porcine reproductive and respiratory syndrome virus replicase, Virus Res. 202 (2015) 48–59.
[9] Y. Fang, E.J. Snijder, The PRRSV replicase: exploring the multifunctionality of an intriguing set of nonstructural proteins, Virus Res. 154 (1–2) (2010) 61–76.
[10] S. Yuan, M.P. Murtaugh, F.A. Schumann, et al., Characterization of heteroclite subgenomic RNAs associated with PRRSV infection, Virus Res. 105 (1) (2004) 75–87.
[11] M.S. Brar, M. Shi, R.K. Hui, et al., Genomic evolution of porcine reproductive and respiratory syndrome virus (PRRSV) isolates revealed by deep sequencing, PLoS One 9 (4) (2014), e88807.
[12] A.E. Firth, J.C. Zevenhoven-Dobbe, N.M. Wills, et al., Discovery of a small arterivirus gene that overlaps the GP5 coding sequence and is important for virus production, J. Gen. Virol. 92 (Pt 5) (2011) 1097–1106.
[13] Y. Li, E.E. Treffers, S. Napthine, et al., Transactivation of programmed ribosomal frameshifting by a viral protein, Proc. Natl. Acad. Sci. U.S.A. 111 (21) (2014) E2172–E2181.
[14] Y. Fang, E.E. Treffers, Y. Li, et al., Efficient -2 frameshifting by mammalian ribosomes to synthesize an additional arterivirus protein, Proc. Natl. Acad. Sci. U.S.A. 109 (43) (2012) E2920–E2928.
[15] C. Huang, Q. Zhang, X.K. Guo, et al., Porcine reproductive and respiratory syndrome virus nonstructural protein 4 antagonizes beta interferon expression by targeting the NF-kappaB essential modulator, J. Virol. 88 (18) (2014) 10934–10945.
[16] J. Dong, S. Xu, J. Wang, et al., Porcine reproductive and respiratory syndrome virus 3C protease cleaves the mitochondrial antiviral signalling complex to antagonize IFN-beta expression, J. Gen. Virol. 96 (10) (2015) 3049–3058.
[17] C. Huang, Y. Du, Z. Yu, et al., Highly pathogenic porcine reproductive and respiratory syndrome virus Nsp4 cleaves VISA to impair antiviral responses mediated by RIG-I-like receptors, Sci. Rep. 6 (2016) 28497.
[18] R. Tao, L. Fang, D. Bai, et al., Porcine reproductive and respiratory syndrome virus nonstructural protein 4 cleaves porcine DCP1a to attenuate its antiviral activity, J. Immunol. 201 (8) (2018) 2345–2353.
[19] Y. Zhao, Z. Song, J. Bai, et al., Porcine reproductive and respiratory syndrome virus Nsp4 cleaves ZAP to antagonize its antiviral activity, Vet. Microbiol. 250 (2020), 108863.
[20] Q. Yang, Q. Zhang, J. Tang, et al., Lipid rafts both in cellular membrane and viral envelope are critical for PRRSV efficient infection, Virology 484 (2015) 170–180.
[21] S. Long, Y. Zhou, D. Bai, et al., Fatty acids regulate porcine reproductive and respiratory syndrome virus infection via the AMPK-ACC1 signaling pathway, Viruses 11 (12) (2019) 1145.
[22] Y. Zhou, Z. Hou, L. Fang, et al., Polyamine regulation of porcine reproductive and respiratory syndrome virus infection depends on spermidine-spermine acetyltransferase 1, Vet. Microbiol. 250 (2020), 108839.
[23] S. Welsch, S. Miller, I. Romero-Brey, et al., Composition and three-dimensional architecture of the dengue virus replication and assembly sites, Cell Host Microbe 5 (4) (2009) 365–375.
[24] C.J. Neufeldt, M. Cortese, E.G. Acosta, et al., Rewiring cellular networks by members of the Flaviviridae family, Nat. Rev. Microbiol. 16 (3) (2018) 125–142.
[25] A. Cambi, F. de Lange, N.M. van Maarseveen, et al., Microdomains of the C-type lectin DC-SIGN are portals for virus entry into dendritic cells, J. Cell Biol. 164 (1) (2004) 145–155.
[26] J. Reyes-Del Valle, S. Chavez-Salinas, F. Medina, et al., Heat shock protein 90 and heat shock protein 70 are components of dengue virus receptor complex in human cells, J. Virol. 79 (8) (2005) 4557–4567.
[27] J.L. Goldstein, M.S. Brown, Regulation of the mevalonate pathway, Nature 343 (6257) (1990) 425–430.
[28] A.K.P. Serquina, D.M. Kambach, O. Sarker, et al., Viral MicroRNAs repress the cholesterol pathway, and 25-hydroxycholesterol inhibits infection, mBio 8 (4) (2017) e00576-17.
[29] Y.J. Li, P. Zhu, Y. Liang, et al., Hepatitis B virus induces expression of cholesterol metabolism-related genes via TLR2 in HepG2 cells, World J. Gastroenterol. 19 (14) (2013) 2262–2269.
[30] J.F. Osuna-Ramos, J.M. Reyes-Ruiz, R.M. Del Angel, The role of host cholesterol during flavivirus infection, Front. Cell. Infect. Microbiol. 8 (2018) 388.
[31] N. Guo, N. Zhang, L. Yan, et al., Down-regulation of single-stranded DNA-binding protein 1 expression induced by HCMV infection promotes lipid accumulation in cells, Braz, J. Med. Biol. Res. 50 (11) (2017) e6389.
[32] Y.P. Ching, T. Kobayashi, S. Tamura, et al., Specificity of different isoforms of protein phosphatase-2A and protein phosphatase-2C studied using site-directed mutagenesis of HMG-CoA reductase, FEBS Lett. 411 (2–3) (1997) 265–268.
[33] J.A. Friesen, V.W. Rodwell, The 3-hydroxy-3-methylglutaryl coenzyme-A (HMG-CoA) reductases, Genome Biol. 5 (11) (2004) 248.
[34] T. Ouyang, G. Niu, Y. Zhang, et al., Porcine HMGCR inhibits porcine circovirus type 2 infection by directly interacting with the viral proteins, Viruses 11 (6) (2019) 544.
[35] X. Yang, F. Chen, Y. Cao, et al., Comparative analysis of different methods to enhance porcine circovirus 2 replication, J. Virol. Methods 187 (2) (2013) 368–371.
[36] R. Soto-Acosta, P. Bautista-Carbajal, M. Cervantes-Salazar, et al., DENV up-regulates the HMG-CoA reductase activity through the impairment of AMPK phosphorylation: a potential antiviral target, PLoS Pathog. 13 (4) (2017), e1006257.
[37] L. Sreelatha, S. Malakar, P. Songprakhon, et al., Serine protease inhibitor AEBSF reduces dengue virus infection via decreased cholesterol synthesis, Virus Res. 271 (2019), 197672.
[38] J.M. Mackenzie, A.A. Khromykh, R.G. Parton, Cholesterol manipulation by West Nile virus perturbs the cellular immune response, Cell Host Microbe 2 (4) (2007) 229–239.

[39] J. Petersen, M.J. Drake, E.A. Bruce, et al., The major cellular sterol regulatory pathway is required for Andes virus infection, PLoS Pathog. 10 (2) (2014), e1003911.
[40] A.G. York, K.J. Williams, J.P. Argus, et al., Limiting cholesterol biosynthetic flux spontaneously engages type I IFN signaling, Cell 163 (7) (2015) 1716–1729.
[41] A. Zhang, H. Duan, H. Zhao, et al., Interferon-induced transmembrane protein 3 is a virus-associated protein which suppresses porcine reproductive and respiratory syndrome virus replication by blocking viral membrane fusion, J. Virol. 94 (24) (2020) e01350-20.
[42] B. Li, L. Fang, S. Liu, et al., The genomic diversity of Chinese porcine reproductive and respiratory syndrome virus isolates from 1996 to 2009, Vet. Microbiol. 146 (3–4) (2010) 226–237.
[43] H. Jing, L. Fang, Z. Ding, et al., Porcine reproductive and respiratory syndrome virus nsp1α inhibits NF-κB activation by targeting the linear ubiquitin chain assembly complex, J. Virol. 91 (3) (2017) e01911–e01916.
[44] J. Chen, D. Wang, Z. Sun, et al., Arterivirus nsp4 antagonizes interferon beta production by proteolytically cleaving NEMO at multiple sites, J. Virol. 93 (12) (2019) e00385-19.
[45] X. Tian, G. Lu, F. Gao, et al., Structure and cleavage specificity of the chymotrypsin-like serine protease (3CLSP/nsp4) of Porcine Reproductive and Respiratory Syndrome Virus (PRRSV), J. Mol. Biol. 392 (4) (2009) 977–993.
[46] F. Guo, V. Stanevich, N. Wlodarchak, et al., Structural basis of PP2A activation by PTPA, an ATP-dependent activation chaperone, Cell Res. 24 (2) (2014) 190–203.
[47] T.H. Chang, J. Segovia, A. Sabbah, et al., Cholesterol-rich lipid rafts are required for release of infectious human respiratory syncytial virus particles, Virology 422 (2) (2012) 205–213.
[48] J.H. Jeon, C. Lee, Cholesterol is important for the entry process of porcine deltacoronavirus, Arch. Virol. 163 (11) (2018) 3119–3124.
[49] M.A. Martin-Acebes, M. Gonzalez-Magaldi, K. Sandvig, et al., Productive entry of type C foot-and-mouth disease virus into susceptible cultured cells requires clathrin and is dependent on the presence of plasma membrane cholesterol, Virology 369 (1) (2007) 105–118.
[50] W. Li, L. Yang, L. Mao, et al., Cholesterol-rich lipid rafts both in cellular and viral membrane are critical for caprine parainfluenza virus type3 entry and infection in host cells, Vet. Microbiol. 248 (2020), 108794.
[51] X.J. Dou, Y. Li, J.L. Han, et al., Cholesterol of lipid rafts is a key determinant for entry and post-entry control of porcine rotavirus infection, BMC Vet. Res. 14 (2018) 45.
[52] A. Pratelli, V. Colao, Critical role of the lipid rafts in caprine herpesvirus type 1 infection in vitro, Virus Res. 211 (2016) 186–193.
[53] J.J. Martin, J. Holguera, L. Sanchez-Felipe, et al., Cholesterol dependence of Newcastle disease virus entry, Biochim. Biophys. Acta Biomembr. 1818 (3) (2012) 753–761.
[54] S. Shanmugam, D. Saravanabalaji, M. Yi, Detergent-resistant membrane association of NS2 and E2 during hepatitis C virus replication, J. Virol. 89 (8) (2015) 4562–4574.
[55] M.O. Trees, B. Londono-Renteria, A. Troupin, et al., Dengue virus reduces expression of low-density lipoprotein receptor-related protein 1 to facilitate replication in Aedes aegypti, Sci. Rep. 9 (2019) 6352.
[56] Y. Sun, S.B. Xiao, D. Wang, et al., Cellular membrane cholesterol is required for porcine reproductive and respiratory syndrome virus entry and release in MARC-145 cells, Sci. China Life Sci. 54 (11) (2011) 1011–1018.
[57] S. Waltl, J.V. Patankar, G. Fauler, et al., 25-Hydroxycholesterol regulates cholesterol homeostasis in the murine CATH.a neuronal cell line, Neurosci. Lett. 539 (2013) 16–21.
[58] E.V. Dang, J.G. McDonald, D.W. Russell, et al., Oxysterol restraint of cholesterol synthesis prevents AIM2 inflammasome activation, Cell 171 (5) (2017) 1057–1071.
[59] H. Dong, L. Zhou, X.N. Ge, et al., Antiviral effect of 25-hydroxycholesterol against porcine reproductive and respiratory syndrome virus in vitro, Antivir. Ther. 23 (5) (2018) 395–404.
[60] Z.B. Song, Q.Y. Zhang, X.W. Liu, et al., Cholesterol 25-hydroxylase is an interferon-inducible factor that protects against porcine reproductive and respiratory syndrome virus infection, Vet. Microbiol. 210 (2017) 153–161.
[61] W. Ke, L. Fang, H. Jing, et al., Cholesterol 25-hydroxylase inhibits porcine reproductive and respiratory syndrome virus replication through enzyme activity-dependent and -independent mechanisms, J. Virol. 91 (19) (2017) e00827-17.
[62] J.W. Song, Y.Y. Liu, P. Gao, et al., Mapping the nonstructural protein interaction network of porcine reproductive and respiratory syndrome virus, J. Virol. 92 (24) (2018) e01112–e01118.
[63] H. Nan, J.X. Lan, M.M. Tian, et al., The network of interactions among porcine reproductive and respiratory syndrome virus non-structural proteins, Front. Microbiol. 9 (2018) 970.
[64] V. Bhatt, K. Shi, D.J. Salamango, et al., Structural basis of host protein hijacking in human T-cell leukemia virus integration, Nat. Commun. 11 (1) (2020) 3121.
[65] W. Chen, R. Possemato, K.T. Campbell, et al., Identification of specific PP2A complexes involved in human cell transformation, Cancer Cell 5 (2) (2004) 127–136.
[66] D. Pim, P. Massimi, S.M. Dilworth, et al., Activation of the protein kinase B pathway by the HPV-16 E7 oncoprotein occurs through a mechanism involving interaction with PP2A, Oncogene 24 (53) (2005) 7830–7838.
[67] T. Kruse, N. Biedenkopf, E.P.T. Hertz, et al., The ebola virus nucleoprotein recruits the host PP2A-B56 phosphatase to activate transcriptional support activity of VP30, Mol. Cell 69 (1) (2018) 136–145 e6.
[68] K. Miyazono, T. Miyakawa, Y. Sawano, et al., Structural basis of abscisic acid signalling, Nature 462 (7273) (2009) 609–614.
[69] K. Kotlo, Y. Xing, S. Lather, et al., PR65A phosphorylation regulates PP2A complex signaling, PLoS One 9 (1) (2014), e85000.
[70] C.M. O'Connor, A. Perl, D. Leonard, et al., Therapeutic targeting of PP2A, Int. J. Biochem. Cell Biol. 96 (2018) 182–193.
[71] J.S. Yu, Activation of protein phosphatase 2A by the Fe2+/ascorbate system, J. Biochem. 124 (1) (1998) 225–230.
[72] A. Kowluru, S.A. Metz, Purine nucleotide- and sugar phosphate-induced inhibition of the carboxyl methylation and catalysis of protein phosphatase-2A in insulin-secreting cells: protection by divalent cations, Biosci. Rep. 18 (4) (1998) 171–186.
[73] S. Galadari, A. Hago, M. Patel, Effects of cations on ceramide-activated protein phosphatase 2A, Exp. Mol. Med. 33 (4) (2001) 240–244.
[74] C. Bernsmeier, F.H.T. Duong, V. Christen, et al., Virus-induced over-expression of protein phosphatase 2A inhibits insulin signalling in chronic hepatitis C, J. Hepatol. 49 (3) (2008) 429–440.
[75] S. Tsunematsu, G. Suda, K. Yamasaki, et al., Hepatitis B virus X protein impairs α-interferon signaling via up-regulation of suppressor of cytokine signaling 3 and protein phosphatase 2A, J. Med. Virol. 89 (2) (2017) 267–275.
[76] A. Garcia, S. Cereghini, E. Sontag, Protein phosphatase 2A and phosphatidylinositol 3-kinase regulate the activity of Sp1-responsive promoters, J. Biol. Chem. 275 (13) (2000) 9385–9389.
[77] E. Sontag, J.M. Sontag, A. Garcia, Protein phosphatase 2A is a critical regulator of protein kinase C zeta signaling targeted by SV40 small t to promote cell growth and NF-kappaB activation, EMBO J. 16 (18) (1997) 5662–5671.
[78] A. Garcia, X. Cayla, E. Sontag, Protein phosphatase 2A: a definite player in viral and parasitic regulation, Microb. Infect. 2 (4) (2000) 401–407.
[79] F. Zhang, P. Gao, X.N. Ge, et al., Critical role of cytochrome c1 and its cleavage in porcine reproductive and respiratory syndrome virus nonstructural protein 4-induced cell apoptosis via interaction with nsp4, J. Integr. Agric. 16 (11) (2017) 2573–2585.
[80] S. Yuan, N. Zhang, L. Xu, et al., Induction of apoptosis by the nonstructural protein 4 and 10 of porcine reproductive and respiratory syndrome virus, PLoS One 11 (6) (2016), e0156518.